crystals

MDPI

Article

High Efficient $YVPO_4$ Luminescent Materials Activated by Europium

Tamara Minakova [1], Sergey Mjakin [2], Vadim Bakhmetyev [2], Maxim Sychov [2], Ilya Zyatikov [3], Irina Ekimova [4], Vladimir Kozik [1], Yu-Wen Chen [5] and Irina Kurzina [1,*]

1 Faculty of Chemistry, National Research Tomsk State University, Tomsk 634050, Russia; tminakova@mail.tomsknet.ru (T.M.); vkozik@mail.ru (V.K.)
2 Department of Theory of Materials Science, Saint-Petersburg State Institute of Technology, Technical University, St. Petersburg 190013, Russia; sergey_mjakin@mail.ru (S.M.); vadim_bakhmetyev@mail.ru (V.B.); materials_science_dept@technolog.edu.ru (M.S.)
3 Laboratory of Gas Lasers, Institute of High Current Electronics SB RAS, Tomsk 634055, Russia; werop@sibmail.com
4 Faculty of Radio Design, Tomsk State University of Control Systems and Radioelektroniks, Tomsk 634050, Russia; ekimova_ira80@mail.ru
5 Department of Chemical Engineering, National Central University, Jhongli 32001, Taiwan; ywchen@cc.ncu.edu.tw
* Correspondence: kurzina99@mail.ru; Tel.: +7-913-882-1028

Received: 22 October 2019; Accepted: 5 December 2019; Published: 9 December 2019

Abstract: YPO_4:Eu, YVO_4:Eu, and $YVPO_4$:Eu based phosphors with various Eu(III) activator contents and phosphate-vanadate ratios were synthesized by the self-propagating high-temperature synthesis method. The samples were characterized by scanning electron microscopy, nitrogen sorption, acid-base indicators and photoluminescence. The particle surface features with a finely dispersed structure comprising all the involved elements. The pore structure and the specific surface areas of the samples were different depending on the compositions of the samples. The most finely dispersed sample was YVO_4:Eu samples. The specific surface areas of the YPO_4:Eu samples were 10 to 15 times greater than those of vanadate samples. The phosphors samples had a slightly basic (YVO_4:Eu, $YVPO_4$:Eu) or slightly acidic (YPO_4:Eu) properties of the surface with different contents of Lewis and Brönsted sites. The differences in the compositions and acid-base state resulted in the difference in the intensity and brightness of the photoluminescence (PL) of the samples. The yttrium-phosphate-vanadate phosphors of the mixed $YV_xP_{1-x}O_4$-Eu had higher brightness and PL intensity than those samples with similar phosphate as well as vanadate phosphors.

Keywords: vanadate-phosphate yttrium phosphors; Eu(III)-activator; surface acidity; photoluminescence

1. Introduction

The development of novel synthetic approaches to oxide phosphors with high luminescence efficiency is one of the most important steps towards various high-tech devices, such as plasma panels, auto-electron emission displays, light sources, thermoluminescent dosimeters, etc. The application in such devices needs specific functional properties of the relating luminescent materials, particularly involving a high quantum yield of luminescence and presence of certain absorption and emission bands. There are many compounds doped with rare-earth ions, the most attractive ones are the oxides of these ions [1–3]. Most of them have high thermal stability and chemical activity. Particularly, phosphors based on rare-earth activated yttrium phosphates and vanadates are some of the most promising compounds of this type [4–11].

These compounds are promising as red-light sources in displays, various light sources providing "warmer" white color for medical applications. These phosphors are obtained by different approaches [4–11] involving hydrolysis in colloids, flow synthesis, solvothermal synthesis, sol-gel techniques, Pechini process, precipitation, hydrothermal synthesis, and microwave heating. The efficiency of the phosphors is determined by the host composition, crystallinity, concentration of structural defects, compositions of the components, distribution uniformity of dopant ion, degree of Y replacement by Eu, specific properties of V and P, as well as the formation of active centers. Therefore, the study of relationships between the synthesis methods/conditions of the materials, compositions, mechanisms of active centers formation, surface features, and luminescence characteristics is an important issue for the development of an approach to adjust their performances and search for optimal preparation conditions.

The aim of this study was to synthesize the phosphors activated by europium, yttrium phosphate and their combinations, and to investigate the relationship between morphology, acid-base properties, and luminescent characteristics of these materials.

2. Materials and Methods

2.1. Synthesis

YVO_4:Eu, YPO_4:Eu as well as mixed $YV_{0.9}P_{0.1}O_4$:Eu [$YVPO_4$(P10):Eu] and $YV_{0.8}P_{0.2}O_4$:Eu [$YVPO_4$(P20:Eu)] phosphors with 0, 5, 7, 8, 10 mol% europium contents, respectively, were prepared by the self-propagating high temperature synthesis (SHS) method according to the procedure described in [12]. Yttrium and europium oxides dissolved in HNO_3 in the calculated ratio reacted with $NH_4H_2VO_4$ or/and $NH_4H_2PO_4$ solutions in the specific ratio with the subsequent evaporation.

The structure of the synthesized samples was confirmed by XRD analysis performed using a Diffray diffractometer. XRD data shown in Figure 1 indicate that the prepared samples correspond to yttrium vanadate structure. The addition of phosphorous results in XRD peak shifting to larger angles due to the formation of YPO_4-YVO_4 solid solution.

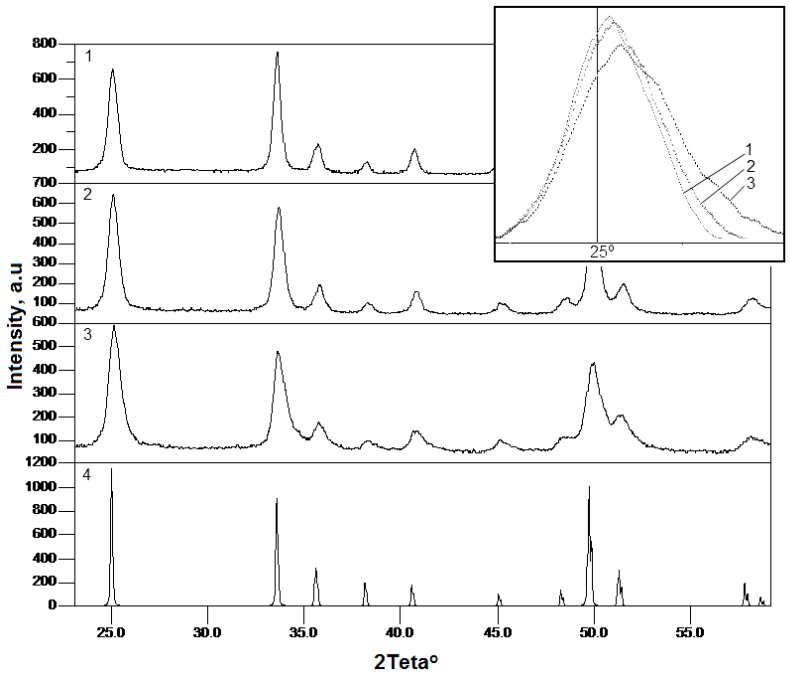

Figure 1. XRD patterns for the samples with phosphorous content 0 (**1**), 10 (**2**) and 20 mol% (**3**) and pattern for the card № 16-250* ICDD PDF database (**4**). The enlarged peak near 25° is shown in the caption to illustrate the effect of phosphorous content.

2.2. Characterization

Porous structure and specific surface area of the prepared phosphors were characterized by BET and BJH methods via low-temperature nitrogen adsorption-desorption using an automated gas adsorption analyzer Micromeritics TriStar II 3020, USA. Degassing of samples was conducted at 200 °C for 2 h [13].

The morphology and particle size of the sample were examined by Scanning Electron Microscopy (Hitachi TM3000, Hitachi, Ltd., Tokyo, Japan) at an accelerating voltage of 15 kV and under the conditions of a charge-off mode from the sample (electron gun: 5×10^{-2} Pa). The nature of the element's distribution on the surface of the samples and the quantitative elemental analysis was carried out on the device for the energy dispersive microanalysis (Quantax 70).

Acid-base properties of the samples were characterized by measuring changes of pH values in bi-distilled water upon suspending a 20 mg sample of the studied material as described in [13–15].

The surface functionality of the phosphors was studied by the adsorption of acid-base indicators with various intrinsic pKa values selectively adsorbing on surface centers with the corresponding pKa with spectrophotometric measurement of the corresponding changes in optical density [14–16] using an SF-56 spectrophotometer (LOMO, St. Petersburg, Russia).

Photoluminescent (PL) performances of the synthesized phosphors were characterized using an SM-2203 spectrofluorimeter (SOLAR, Belarus). The recorded luminescence spectra were analyzed to determine the number and positions of maximum in the excitation and luminescence spectra, intensity and FWHM level corresponding to 50% photoluminescence intensity relating to the maximum intensity. Photoluminescent (PL) performances of the synthesized phosphors were characterized using an SM-2203 spectrofluorimeter (SOLAR, Belarus). The recorded luminescence spectra were analyzed to determine the number and positions of maximums (max) in the excitation and luminescence spectra, intensity (I) and FWHM level corresponding to 50% photoluminescence intensity relating to the maximum intensity. The excitation spectra were recorded upon the adjustment of the excitation monochromator Ex to a certain wavelength range and fixing the emission monochromator Em at the selected wavelength. The luminescence spectra were recorded upon fixing Ex at the target excitation wavelength and Em was used for scanning over the emission wavelength range [8,17].

The exciting light of the radiation source (high-pressure xenon arc lamp DKsSh 150-1M, (Zelenograd, Moscow, Russia) fell on the sample perpendicular to its surface, and luminescence was recorded at an angle of 450, which reduced the contribution of reflected light from the radiation source. We used a holder for solid samples with a gap of 2.2, a step of 1 nm, and a medium velocity. The excitation spectra of samples activated by europium ions have maxima in the range of 320–336 nm.

The luminescence brightness of the phosphors was measured using an IL1700 research radiometer (International Light Technologies, Inc., Peabody, MA, USA) at optimal wavelengths for both materials (286 nm for YVO_4 based phosphors and 365 nm for YPO_4 based ones). Investigated the phosphor is filled in the cell. When the UV lamp is off, the radiometer readings are set to zero. After that, the lamp turns on, the cuvette with the phosphor is placed in the box, the shutter closes, and the readings of the radiometer are read [18].

3. Results and Discussion

3.1. Pore Structure

The data of low-temperature nitrogen adsorption/ for the sample YPO_4:Eu(8) shown in Figure 2 feature with a prominent hysteresis that suggests a capillary condensation in the pores. Processing of these data using BET equation at P/P_0 = 0.05–0.35 gives the specific surface 83 m^2/g, whereas treatment according to Thomson-Kelvin equation indicates that this sample is mesoporous with the pore sizes ranging from 4 to 6 nm and the average pore volume V_{pore} about 0.13 cm^3/g.

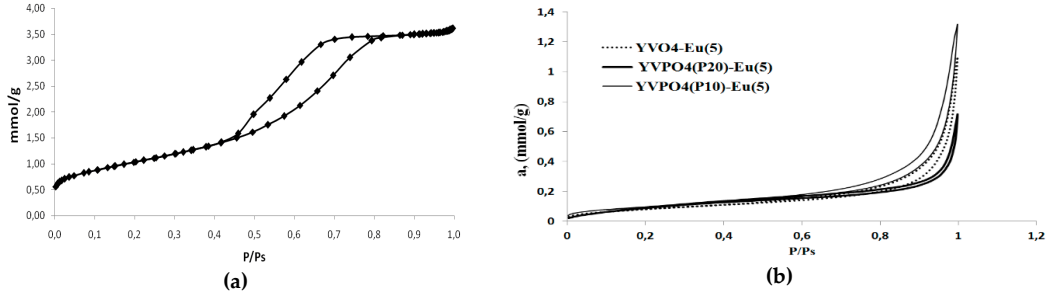

Figure 2. Isotherms of nitrogen adsorption-desorption for the samples (**a**) YPO_4:Eu (8); (**b**) $YV_{0.9}P_{0.1}O_4$:Eu (5), $YV_{0.8}P_{0.2}O_4$:Eu (5), and YVO_4:Eu (5).

The porous structure and adsorptive properties of the studied phosphors are summarized in Table 1.

Table 1. Pore structure and adsorptive properties of the phosphors.

Sample	S_{BET} (m^2/g)	V_{pore} (m^3/g)	Monolayer Adsorption a_m (mmol/m^2)	Adsorption Value at $P/P_0 = 1$ (mmol/m^2)
YPO_4:Eu(8)	83	0.13	0.85	3.7
YPO_4:Eu(5)	90	0.15	0.92	4.3
YVO_4:Eu(5)	6	0.04	0.07	1.1
$YV_{0.9}P_{0.1}O_4$:Eu (5)	8	0.05	0.08	1.3
$YV_{0.8}P_{0.2}O_4$:Eu (5)	9	0.03	0.09	0.7

YPO_4:Eu (5% and 8%) samples are also mesoporous with pore sizes 4–10 nm. On the contrary, the phosphors based on yttrium vanadate and mixed vanadate-phosphate are nonporous (contain only a small number of large mesopores), as indicated by adsorption isotherms and small the specific surface values.

3.2. SEM

SEM photos of YVO_4:Eu (0%, 5%, 8%), YPO_4:Eu (0%, 5%, 8%), $YV_{0.9}P_{0.1}O_4$:Eu (0%, 5%, 8%) and $YV_{0.8}P_{0.2}O_4$:Eu (0%, 5%, 8%) shown in Figure 3 samples suggest their polydispersity with well-defined small particles of 1–4 μm and agglomerates (tens of micrometers). The largest agglomerates (up to 150 μm) are observed for YPO_4-based phosphors, while the most finely dispersed samples are based on YVO_4 and mixed $YV_xP_{1-x}O_4$:Eu phosphors comprise the particles of intermediate size and agglomerate size below 20 μm. The average size of europium-free YPO_4, YVO_4, and $YV_xP_{1-x}O_4$ samples were 1.5–3, 1–2, and 1.7–2.5 μm, respectively.

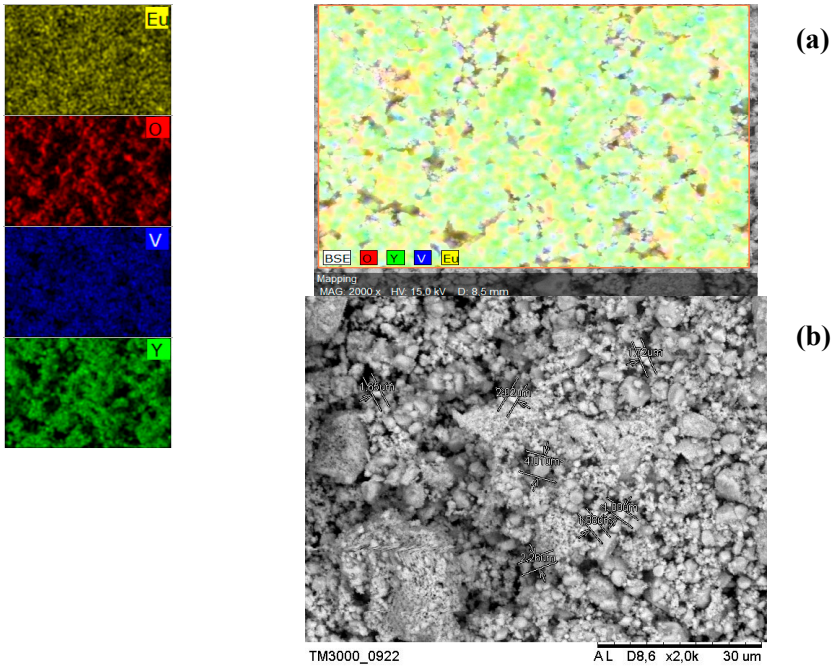

Figure 3. Elements distribution profile on the surface of YVO_4:Eu(8) phosphor (**a**); surface morphology YVO_4:Eu(8) (**b**).

The elemental analysis based on the element distribution profiles and energy spectra for YVO_4:Eu(8) phosphor sample is shown in Figure 3. It clearly shows uniform distributions of all elements on the surface. All samples show the same uniform elemental distribution.

The contents of various elements on the phosphor surface are tabulated in Table 2 for the samples with Eu content 8 mol%. The results of other samples featured with similar ratios.

Table 2. Element contents on the surface of samples with Eu content 8 mol%.

Sample	**YVO_4:Eu(8)**		**YPO_4:Eu(8)**		**$YV_{0.9}P_{0.1}O_4$:Eu(8)**	
Elements	**[norm. wt.%]**	**[norm. at.%]**	**[norm. wt.%]**	**[norm. at.%]**	**[norm. wt.%]**	**[norm. at.%]**
Oxygen	17.08	48.41	17.08	48.41	18.46	49.75
Yttrium	49.61	25.30	27.65	24.61	48.60	23.57
Vanadium	27.65	24.70	0	0	24.35	20.61
Europium	5.66	1.69	5.66	1.69	5.31	1.51
Phosphorous	0	0	17.06	17.23	3.28	4.57

EDX results for YVO_4, YPO_4, $YV_{0.9}P_{0.1}O_4$, and $YV_{0.8}P_{0.2}O_4$ based phosphors with Eu contents 0, 5, and 8 mol%, respectively, demonstrate a uniform distribution of all the components on the surface, suggesting a single phase in the samples.

3.3. Acid-Basic Properties of the Samples

The dispersity, chemical compositions, and the imperfection of the crystal structure affect the state of the surface, which is reflected in the acid-base and luminescence properties of the crystal phosphors. The change of pH value for the aqueous medium after immersing the samples until the equilibrated isoionic state (iis) are presented in Figure 4. The pH_{iis} results indicate a weak acidity on YPO_4-based samples and weak basicity on the YVO^{4-} and $YV_{0.9}P_{0.1}O_4$–based samples. The presence of europium slightly modified the surface to basicity.

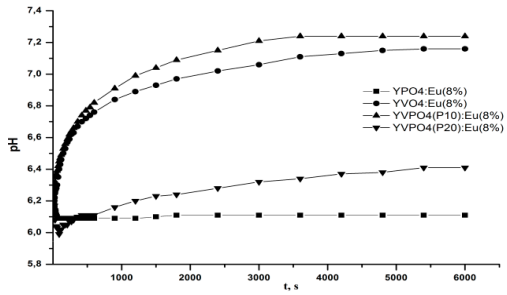

Figure 4. pH change in aqueous slurries of the samples with europium content 8 mol%.

The initial period straight after the suspending of the sample's features with the most significant pH changes, followed by a trend to saturation. pH drops sharply to a minimum for YPO_4-based samples a predominantly occupation of their surface with Lewis acidic centers (probably corresponding to phosphorous atoms) featuring with a rapid interaction with water. The subsequent slight increase of pH indicates the participation of Brönsted acidic hydroxyl. For YVO_4 and $YV_{0.9}P_{0.1}O_4$-based phosphors, a steady pH growth was observed in the initial phase that suggests the presence of both Lewis and Brönsted basic centers.

Figure 5 shows the change in the total surface acidity of yttrium phosphate, yttrium vanadate, and mixed samples. The smooth increase in the surface acidity from YVO_4 to YPO_4 is in accordance with the chemical properties of these compounds. It can be seen in Table 3 that activation by europium ions changed the pHiis parameter. The dependence is not unique, however, the regularity in the change in total acidity persists for the samples with the same percentage of europium (5 or 8) was observed. Phosphor plays a crucial role in these samples.

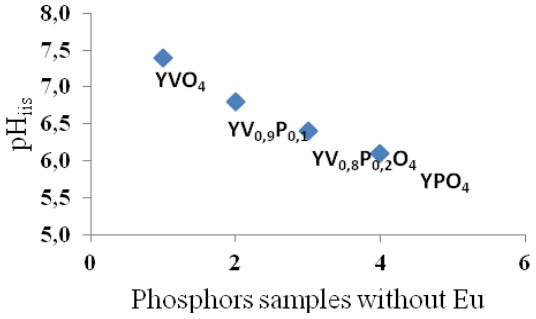

Figure 5. Change in surface acidity for yttrium phosphate, yttrium vanadate, and mixed samples.

Table 3. pH change kintetics in aqueous slurries of the samples with Eucountent 0, 5 and 8 mol%.

Sample	PH_0	pH_{IIS}	Sample	PH_0	pH_{IIS}
YPO_4:Eu(0)	6.4	6.1	$YVPO_4$(P10):Eu(0)	6.4	6.8
YPO_4:Eu(5)		5.7	$YVPO_4$(P10):Eu(5)		6.5
YPO_4:Eu(8)		6.1	$YVPO_4$(P10):Eu(8)		6.9
YVO_4:Eu(0)		7.4	$YVPO_4$(P20):Eu(0)		6.4
YVO_4:Eu(5)		7.5	$YVPO_4$(P20):Eu(5)		6.4
YVO_4:Eu(8)		7.2	$YVPO_4$(P20):Eu(8)		6.4

The study of the prepared materials by the adsorption of acid-base indicators (Figure 6) indicates that the surface of Eu-free YVO_4 features with a relatively low content of adsorption centers, whereas the addition of europium results in a drastic increase in the content of different sites, particularly with pK_a −4.4 (7% Eu), −0.9 and 1.3 (5% Eu), 2.5 and 5 (5–10% Eu), 7 . . . 9 (5% Eu) and 14.2 (5, 10 and 8% Eu).

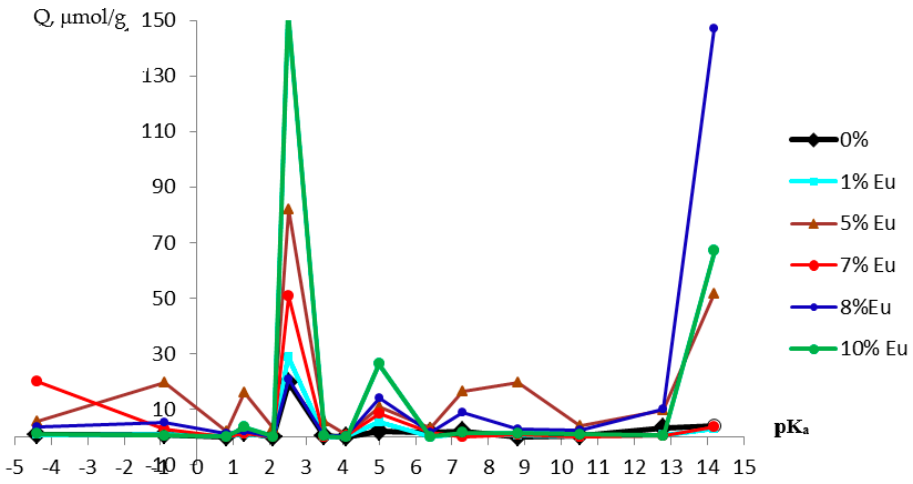

Figure 6. Distribution of adsorption centers on the surface of $Y_{1-x}VO_4:Eu_x$ samples.

Europium concentration clearly correlates with the content of adsorption centers with pK_a 5.0 (Figure 7) probably corresponding to weakly acidic hydroxyl groups formed due to the distortion of element-oxygen bonds in the surface layer.

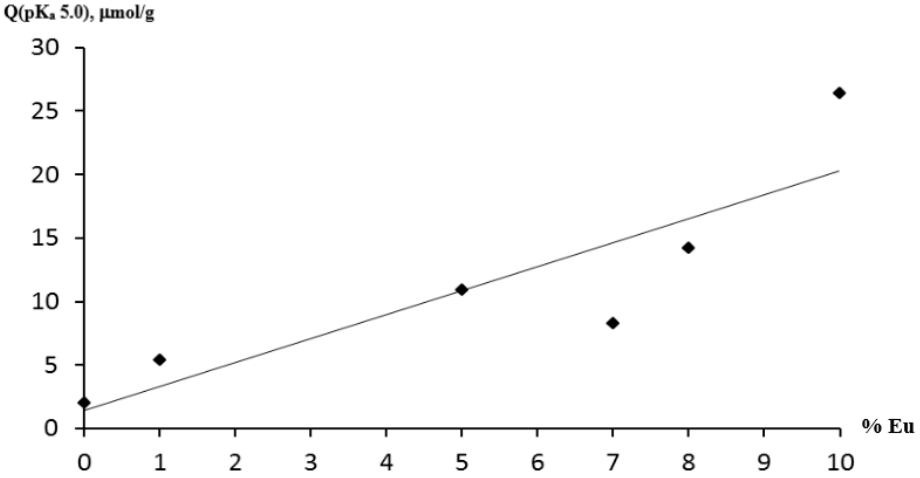

Figure 7. Content of centers with pK_a 5.0 on the surface of $Y_{1-x}VO_4:Eu_x$ phosphors. as a function of europium content.

Generally, the surface acidity of the considered samples increased in the order: YVO_4:Eu < $YVPO_4$(P10):Eu < $YVPO_4$(P20):Eu < YPO_4:Eu, that is in agreement with indicator adsorption data (Figures 8 and 9).

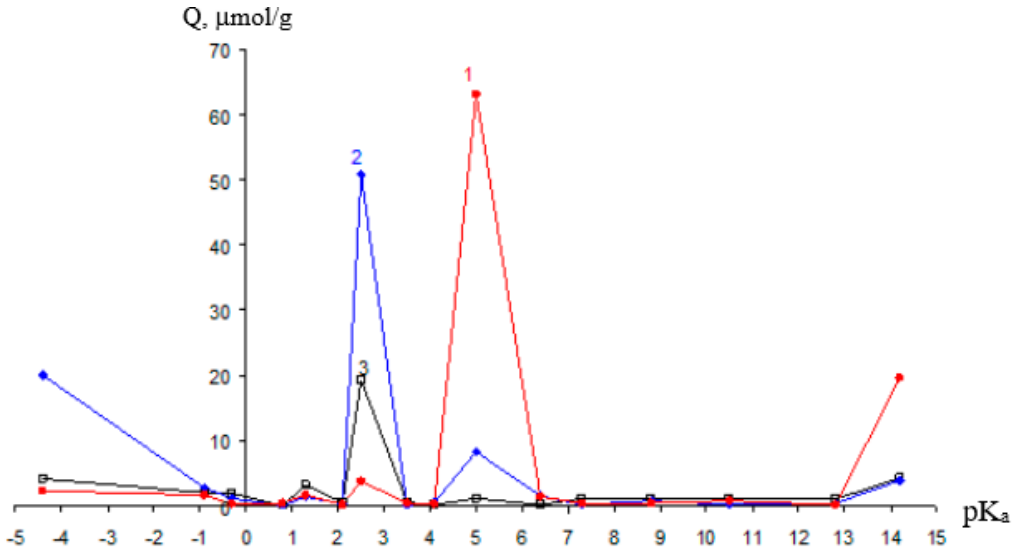

Figure 8. Distribution of adsorption sites on the surface of $Y_{0.93}V_{0.2}P_{0.8}O_4$:$Eu_{0.07}$ (1) in comparison with the phosphors based on YVO_4 (2) and YPO_4 (Eu 7 mol%) (3).

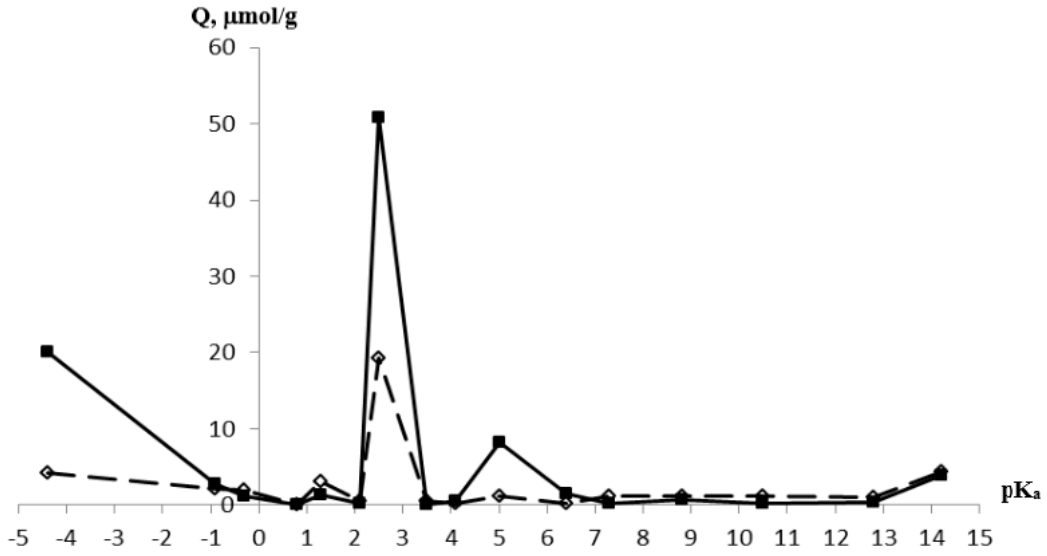

Figure 9. Distribution of adsorption sites on the surface of YVO_4:Eu (solid line) and YPO_4:Eu (dashed) samples with Eu content 7 mol%.

Furthermore, comparative data for the distributions of adsorption centers (Figures 8 and 9) indicate that the contents of Lewis acidic centers (LAC) with pK_a 14.2 increased in the order of YVO_4:Eu < $YV_{0.9}P_{0.1}O_4$:Eu < YPO_4:Eu, confirming the results of acidities from pH-metric data. According to the earlier studies [14,15], such centers relating to oxygen vacancies or surface cations deteriorate the luminescence performances due to their ability to electron trapping, however, their transition into Brönsted sites (particularly hydroxyls with pK_a 2.5) leads to the increase in luminescence characteristic. Instead, an increase in the concentration of Lewis base sites in the opposite row leads to an increase in the photoluminescence intensity.

The considered differences in acid-base properties of the studied samples surface can be attributed to relatively high acidity and low size of phosphorous atoms promoting their localization on the surface, whereas V ions are keener towards hydroxylation.

3.4. Excitation and Luminescence

The excitation and luminescence spectra of the phosphors samples and their luminescence brightness as a function of europium content are shown in Figures 10 and 11. The luminescence performances of the phosphors materials are summarized in Table 4.

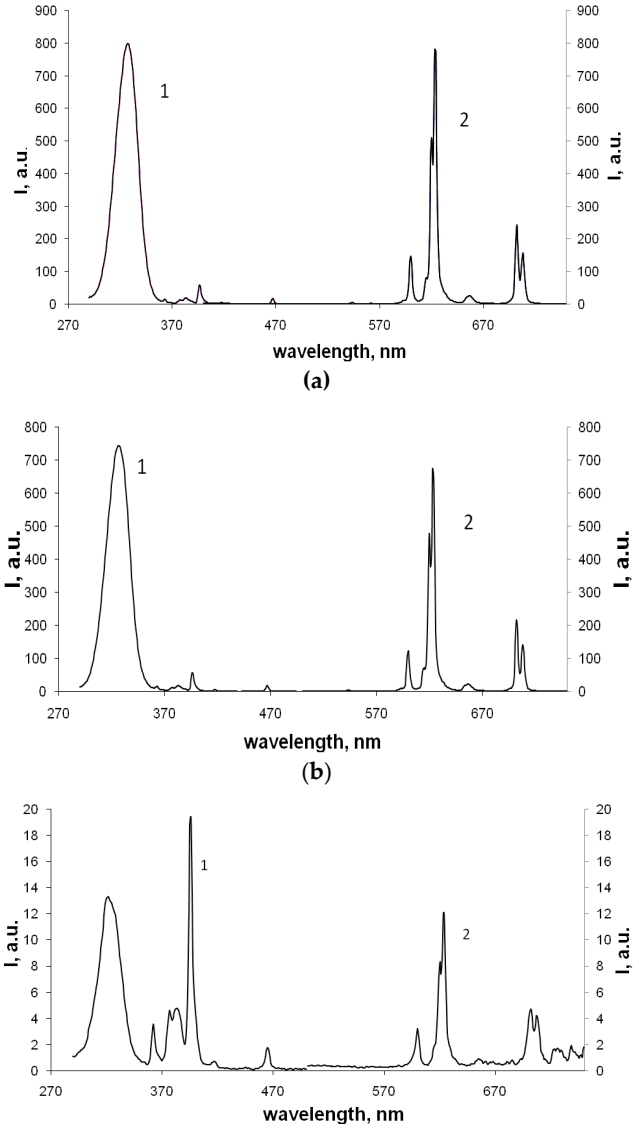

Figure 10. Excitation (1) and luminescence (2) spectra for (**a**) $YV_{0.9}P_{0.1}O_4$:Eu(8); (**b**) YVO_4Eu(10), and (**c**) YPO_4Eu(10) phosphors.

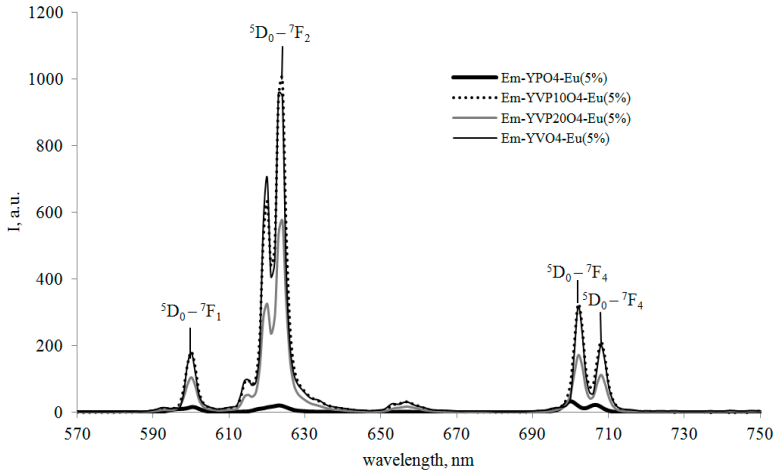

Figure 11. PL spectra of the phosphors with 5% europium content.

Table 4. Luminescence performances of the phosphors.

Sample	Composition		Excitation Band Peaks, nm			Emission Band Peaks, nm	
	Host Material	Eu Content, mol%	λ_{lum} = 623 nm	I, a.u.	I_{327}/I_{396}	λ_{ex} = 328 nm	I, a.u.
1	$YVPO_4$ P10	8	327	799	14	623	781
			396	58			
2	YVO_4	10	327	744	13	624	673
			396	56			
3	YPO_4	10	322	13	0,7	623	11
			396	19			

The excitation spectra of all Eu(III) activated samples are similar to each other featuring with an intensive short wavelength band λ_{max} = 327 nm commonly accounted for charge transfer transitions from O^{2-} to Eu^{3+} ($O^2p \rightarrow Eu^4f$). In addition, a set of low intensity narrow bands were observed in the region 350-500 nm relating to Eu ion intra configuration 4f-4f-transitions $^7F^0$–$^5D_4$, $^7F^0$–$^5G_2$, $^7F^0$–$^5L_6$, $^7F^0$–$^5D_3$, $^7F^0$–$^5D_2$ with respective peaks at 362, 382, 396, 412 and 466 nm. The intensity of the short-wave bands with maxima at 327 nm is significantly higher than the intensity of the most pronounced band in the excitation spectrum of the Eu^{3+} with a maximum at 396 nm for the samples $YV_{0.9}P_{0.1}O_4$:Eu(8) and YVO_4:Eu(10) (Figure 10a,b and Table 4). The intensity of the short-wave band is weaker than those in the previous samples for the YPO_4:Eu(10) excitation spectra. The intensity of the bands due to the transitions of Eu^{3+} ion was high.

For $YV_{0.9}P_{0.1}O_4$:Eu(8) and YVO_4:Eu(10) samples, the intensity of bands at 327 nm was significantly higher that of 394 nm (Table 4). In the vanadium-free YPO_4:Eu(10) phosphor sample, the intensity of short wave band at 322 nm was very low (I_{327}/I_{396} = 0,7), indicating unfavorable conditions for $O^{2-} \rightarrow Eu^{3+}$ charge transfer in this sample.

The PL spectra of the studied Eu(III) activated phosphors are almost the same featuring with bands corresponding to transitions from $^5D_0$ metastable level to the basic multiplet level ^7Fj of Eu^{3+} ion with wavelength maxima at 600, 620. 623, 702, and 708 nm. The intensities of the bands depend on the europium content, but this is ambiguous. In the case of $YVPO_4$ P10 phosphor, the intensity decreased with an increase in europium content, and an inverse relationship was observed for the remaining phosphors. The most intensive band with the maximum at 623 nm relates to $^5D_0 \rightarrow ^7F_2$ transition. The highest luminescence intensity was observed for $YV_{0.9}P_{0.1}O_4$:Eu(8) and YVO_4:Eu(10) samples, about 60 times exceeding the value for YPO_4:Eu(10) (Table 4).

In the spectra of these phosphors, the absence of a short-wave band with the maximum at 462 nm relating to the host material luminescence is probably due to the absorbed energy transfer from the host matrix to Eu ions. In conclusion, the host material composition is one of the significant factors affecting the PL intensity of Eu(III) ions.

The comparison characteristic of peaks intensities in luminescent spectra for $YV_{0.9}P_{0.1}O_4$:Eu(8), YVO_4Eu(8), and YPO_4Eru(8) phosphors, obtained at the excitation wavelength of 305 nm (λ_{ex}) is shown in Figure 12, while the gap was 1-1. Thus, one of the factor, that influence on the PL intensity of Eu(III) ions under the same research conditions is probably the matrix composition.

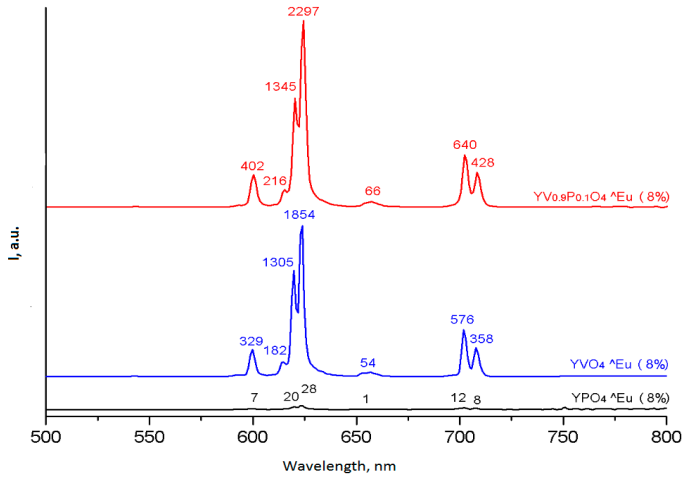

Figure 12. PL spectra of the phosphors with 8% europium content.

As shown in Figure 13, the luminescence brightness of almost all the studied phosphors passes through the maximum at Eu content 7 mol% (x = 0.07). At this optimal Eu content, the highest brightness is observed for the mixed vanadate-phosphate sample with phosphorous content 10 mol%. and for the sample with 20 mol % P the brightness is almost the same as for the pure YVO_4 based phosphor.

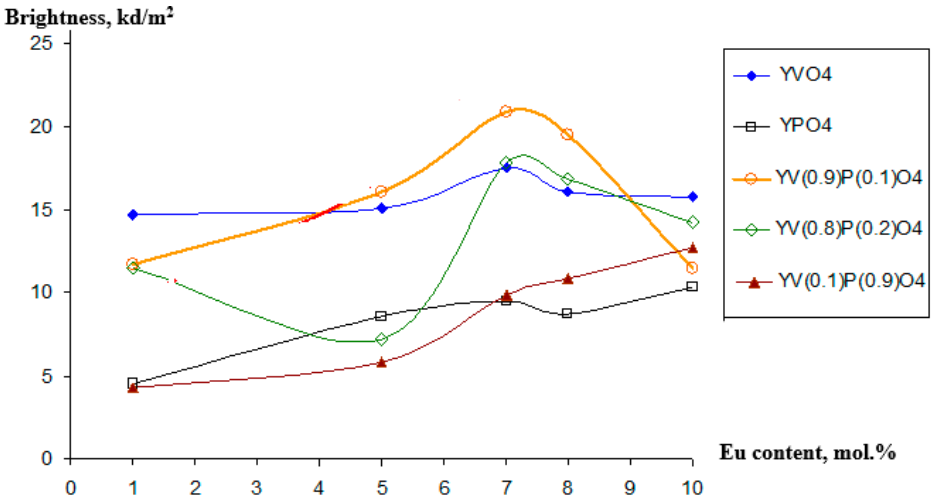

Figure 13. Luminescence brightness of vanadate-, phosphate, and mixed vanadate-phosphate based phosphors as a function of Eu content.

The comparison of these data with the phosphor surface functionality (Figure 6) shows that the sample with Eu content 7 mol% providing the highest luminescence brightness features with the highest content of Lewis basic centers with pK_a −4.4 in couple with a reduced content of Brönsted basic sites with pKa 7 . . . 13 and absence of Lewis acidic centers with pK_a 14.2 (i.e. “electron traps” preventing

from luminescent electron transitions). The considered functionality likely reflects the structural perfection of the surface predominantly occupied with V=O or P=O groups (and, consequently, oxygen atoms) intrinsic to vanadate structure.

In this study, much attention was paid to the investigation of the phosphors surface properties without a detailed consideration of the effect of the matrix structure on the corresponding luminescent transitions. In the previous studies [19–21], we have shown that acid-base active sites, dispersity, and porosity reflect the imperfection of the solids surface structure and affect the luminescent properties of materials sensitive to the surface state. This study shows that the phosphors based on YVO_4 had more intense PL and increased brightness compared with the samples based on YPO_4.

In addition, they are distinguished by a more basic surface state ($pH_{iis} > 7$), a small value of the specific surface area, and low porosity. Phosphate phosphors have an acidic surface, a large value of the specific surface area, narrow mesoporous size distribution, and predominance of Lewis acid sites on the surface, in comparison with vanadate samples on the surface of which the Lewis base sites predominate. Phosphors based on yttrium phosphates are less photoluminescent active than the phosphors based on yttrium vanadate.

The results of this study infer that the increased brightness of YVO_4 based phosphors relating to YPO_4 based samples correlates with a decrease concentration of Lewis acidic centers, probably corresponding to the surface P or V atoms featuring with electron-accepting (or "electron trapping") properties preventing from luminescent electron transitions. Phosphorous atoms possess higher acidity and tendency to localization on the surface than the vanadium due to lower size, while V is capable to coordinate more oxygen atoms blocking such undesirable Lewis acid sites and either forming bridging bonds between ions to stabilize the surface compounds facilitating the luminescence increase or yielding Brönsted sites (hydroxyl groups) present on the surface of vanadate samples in a significantly higher amount. Furthermore, a high concentration of Lewis acid sites on the surface of yttrium phosphate-based samples can be responsible for their tendency to agglomeration due to strong interparticle interactions, that also contributes to reduced PL brightness correlating with the overall surface activated by UV radiation to stimulate luminescence.

In summary, the synthesis of mixed yttrium vanadate-phosphate phosphors provides an increase in PL brightness compared with both individual components due to their interphase interactions yielding new surface compounds. This approach is promising for the further optimization of the compositions of the phosphors to improve their performance [20–22].

4. Conclusions

A series of YPO_4:Eu, YVO_4:Eu and $YVPO_4$:Eu phosphors with different contents of Eu(III) activator and with different phosphorus-vanadium ratios for the mixed phosphors were synthesized by SHS technique. The host material composition in Eu(III)-activated YVO_4, YPO_4 and mixed $YV_{1-x}P_xO_4$ based phosphors significantly affected their luminescence performances due to the differences in matrix structure as well as the surface acid-base properties and functional composition. YPO_4 based phosphors provided much lower photoluminescence intensity and brightness than the YVO_4 analogs, due to finely mesoporous nature, higher specific surface area, stronger acidity and more reactive surface by a large content of Lewis acidic sites featuring with "electron trapping" properties hampering luminescent electron transitions and facilitating particle agglomeration. Although the luminescence brightness of a pure YPO_4 based phosphor is much lower compared to YVO_4 based analog, a partial (10%) replacement of vanadium by phosphorous provides a considerable brightness increase compared with a pure vanadate-based material. Furthermore, this effect is promising in respect of cost reduction for the considered phosphors. The optimal europium content 7 mol% providing the highest luminescence brightness for both vanadate- and mixed vanadate-phosphate phosphors is determined and found to correlate with the lowest content of "electron trapping" centers, prevailing of oxygen centers corresponding to V=O groups and reflecting the most perfect surface structure.

Author Contributions: T.M. conceived the experiment, interpreted the specific surface area results and wrote the paper, S.M. performed and interpreted the adsorption experiments, V.B. performed and interpreted the luminescence performances of the samples, M.S. performed and interpreted the observed pH changes in aqueous slurries after suspending the samples, V.K. performed and interpreted the SEM and EPMA and wrote the paper, I.E. interpreted distribution of adsorption sites on the surface of samples, Y.-W.C. performed pH measurement in aqueous slurries of the samples, I.Z. synthesized samples. All authors reviewed the manuscript.

Funding: This research was supported by the Program of Increasing the Competitiveness of TSU № 8.10.2. 2018.

Conflicts of Interest: The authors declare no conflict of interest.

References

1. Luwang, M.N.; Ningthoujam, R.S.; Srivastava, S.K.; Vatsa, R.K. Preparation of white light emitting YVO_4:Ln^{3+} and silica-coated YVO_4:Ln^{3+} (Ln^{3+}, Eu^{3+}, Dy^{3+}, Tm^{3+}) nanoparticles by CTAB/n-butanol/hexane/water microemulsion route: Energy transfer and site symmetry studies. *J. Mater. Chem. R. Soc. Chem.* **2011**, *21*, 5326–5337. [CrossRef]
2. Muenchausen, R.E.; Jacobsohn, L.G.; Bennett, B.L.; McKigney, E.A.; Smith, J.F.; Valdez, J.A.; Cooke, D.W. Effects of Tb doping on the photoluminescence of Y_2O_3: Tb nanophosphors. *J. Lumin.* **2007**, *126*, 838–842. [CrossRef]
3. Sun, H.; Peng, D.; Wang, X.; Tang, M.; Zhang, Q.; Yao, X. Strong red emission in Pr doped $(Bi_{0.5}Na_{0.5})TiO_3$ ferroelectric ceramics. *J. Appl. Phys. AIP Publ.* **2011**, *110*, 161–172. [CrossRef]
4. Kumari, P.; Baitha, P.K.; Manam, J. Structural and photoluminescence properties of red-light emitting YVO_4:Eu^{3+} phosphor synthesized by combustion and solid-state reaction techniques: A comparative study. *Indian J. Phys.* **2015**, *89*, 1297–1306. [CrossRef]
5. Zhang, F.; Zhang, W.; Zhang, Z.; Huang, Y.; Tao, Y. Luminescence characteristics and energy transfer of a red-emitting YVO_4:Sm^{3+}, Eu^{3+} phosphor. *J. Lumin.* **2014**, *152*, 160–164. [CrossRef]
6. Luo, Q.; Shen, S.; Lu, G.; Xiao, X.; Mao, D.; Wang, Y. Synthesis of cubic ordered mesoporous YPO_4:Ln^{3+} and their photoluminescence properties. *J. Mater. Chem.* **2009**, *19*, 8079–8085. [CrossRef]
7. Tymiński, A.; Grzyb, T. Enhancement of the up-conversion luminescence in $LaVO_4$ nanomaterials by doping with M^{2+}, M^{4+} (M^{2+} = Sr^{2+}, Ba^{2+}, Mg^{2+}; M^{4+} = Sn^{4+}) ions. *J. Alloys Compd.* **2019**, *782*, 69–80. [CrossRef]
8. Bhatkar, V.B. Synthesis and luminescent properties of yttrium vanadate based phosphors. *Int. J. Eng. Sci. Innov. Technol.* **2013**, *2*, 426–429.
9. Cavalli, E.; Angiuli, F.; Belletti, A.; Boutinaud, P. Luminescent spectroscopy of YVO_4:Ln^{3+}, Bi^{3+} (Ln^{3+} = Eu^{3+}, Sm^{3+}, Dy^{3+}) phosphors. *Opt. Mater.* **2014**, *36*, 1642–1648. [CrossRef]
10. Zhiguo, X.; Daimein, C.; Min, Y.; Ting, Y. Synthesis and luminescence properties of YVO_4:Eu^{3+}, Bi^{3+} phosphor with enhanced photoluminescence by Bi^{3+} doping. *J. Phys. Chem. Solids* **2010**, *71*, 175–180.
11. Su, X.Q.; Yan, B. The synthesis and luminescence of $YP_xV_{1-x}O_4$: Dy^{3+} microcrystalline phosphors by in situ co-precipitation composition of hybrid precursors. *Mater. Chem. Phys.* **2005**, *93*, 552–556. [CrossRef]
12. Minakova, T.; Eremina, N.; Mjakin, S.; Bakhmetyev, V.; Sychov, M.; Svatovskaya, L.; Dolzhenko, D.; Sychova, A. Dispersity and Surface Characterization of Yttrium Vanadate and Phosphate Based Luminescent Phosphors. In Proceedings of the 2018 IEEE International Conference on Electrical Engineering and Photonics (EExPolytech-2018), Saint Petersburg, Russia, 22–23 October 2018.
13. Karnaukhov, A.P. *Adsorption. Texture of Dispersed and Porous Materials*; Science: Novosibirsk, Russia, 1999.
14. Minakova, T.S. *Adsorbzionnye Prozessy na Poverhnosti Tverdykh tel (Adsorption Processes on the Surface of Solids)*; Tomsk University: Tomsk, Russian, 2007.
15. Sychov, M.M.; Minakova, T.S.; Slizhov, Y.G.; Shilova, O.A. *Kislotno-Osnovnye Kharakteristiki Poverhnosti Tverdykh tel I Upravlenie Svoistvami Materialov I Kompozitov (Acid-Base Properties of Solids and Control over the Properties of Materials and Composites)*; Khimizdat Publishers: St. Petersburg, Russia, 2016.
16. Nechiporenko, A.P. *Donorno-Akzeptornye Svoistva Poverhnosti Tverdofaznyh Sistem. Indikatornyi Metod (Acid-Base Properties of Solid Phase Systems; Indicator method)*; Lan Publishers: St. Petersburg, Russia, 2017.
17. Mjakin, S.V.; Sychov, M.M.; Vasiljeva, I.V. *Electron Beam Modification of Solids: Mechanisms, Common Features and Promising Applications*; Nova Science Publishers, Inc.: Hauppauge, NY, USA, 2009.
18. Lebedev, L.A.; Mjakin, S.V.; Nikandrova, A.A.; Bakhmetyev, V.V.; Sychov, M.M. Study of luminescence and surface properties of $Y_{1-x}Eu_xV_{1-y}PyO_4$ phosphors. *Smart Nanocomposites* **2016**, *13*, 15–20.

19. Minakova, T.S.; Sychov, M.M.; Bakhmetyev, V.V.; Eremina, N.S.; Bogdanov, S.P.; Zyatikov, I.A.; Minakova, L.Y. The Influence of $Zn_3(PO_4)_2$:Mn-Luminophores Synthesis Conditions on their Surface and Luminescent Features. *Adv. Mater. Res.* **2014**, *872*, 106–111. [CrossRef]
20. Ekimova, I.; Minakova, T.; Ogneva, T. Phisicochemistry of Alkaline-Earth Metals Oxides Surface. *AIP Conf. Proc.* **2016**, *1698*, 060014.
21. Bakhmetyev, V.V.; Lebedev, L.A.; Vlasenko, A.B.; Bogdanov, S.P.; Sovestnov, A.E.; Minakova, T.S.; Minakova, L.Y.; Sychov, M.M. Luminescent Materials on the Basis of Yttrium Oxide and Yttrium Aluminum Garnet Used for Photodynamic Therapy. *Key Eng. Mater.* **2015**, *670*, 232–238. [CrossRef]
22. Xiong, H.; Zhang, Y.; Liu, Y.; Gao, T.; Zhang, L.; Qiao, Z.A.; Zhang, L.; Gan, S.; Huo, Q. Self-template construction of honeycomb-like mesoporous YPO_4:Ln^{3+} (Ln = Eu, Tb) phosphors with tuneable luminescent properties. *J. Alloys Compd.* **2019**, *25*, 845–851. [CrossRef]

© 2019 by the authors. Licensee MDPI, Basel, Switzerland. This article is an open access article distributed under the terms and conditions of the Creative Commons Attribution (CC BY) license (http://creativecommons.org/licenses/by/4.0/).